*Int. J. Heat Mass Transfer.* Vol. 18, pp. 477–493. Pergamon Press 1975. Printed in Great Britain

# THE GROWTH OF VAPOR BUBBLES IN SUPERHEATED SODIUM*

M. DALLE DONNE† and M. P. FERRANTI†
Gesellschaft für Kernforschung mbH., Karlsruhe, West Germany

(*Received* 21 *December* 1973 *and in revised form* 21 *June* 1974)

**Abstract**—It is known from experiments that the degree of incipient boiling superheat can be considerably higher with sodium than with water. The expanding bubble experiences large temperature differences. This, together with the fact that thermal diffusivity of the liquid sodium is much higher than that of water, is the reason why the Plesset–Zwick asymptotic solution is valid for sodium only for very low superheats. In the present work a way to numerically integrate the relevant differential equations with the computer code HY-BUBBLE is shown. Results for sodium with superheats up to 380°C are given. Comparison of HY-BUBBLE calculations for water with relatively high degrees of superheat with experiments of Cole and Shulman and of Kosky show good agreement. HY-BUBBLE calculations cannot predict the experiments of Hooper and Abdelmessih for water with high degrees of superheat.

## NOMENCLATURE

$b$, heat produced in the liquid per unit volume and time [cal/cm³ s];
$c$, specific heat of the liquid [cal/g °K];
$D$, liquid thermal diffusivity [cm²/s];
$e$, energy that a radiation particle loses per unit track [cal/cm];
$h$, $= \frac{1}{3}(r^3 - R^3(t))$ [cm³];
$k$, thermal conductivity of the liquid [cal/cm s °K];
$J$, conversion factor from work units to heat units [dyn . cm/cal];
$L$, latent heat of vaporisation [cal/g];
$N$, number of atoms per unit volume [cm⁻³];
$N_{Ja}$, $= \dfrac{\rho c(T_0 - T_s)}{\rho_v(T_s)L(T_s)}$ Jakob number;
$N'_{Ja}$, $= \dfrac{\rho c(T_0 - T)}{\rho_v(T)L(T)}$ transient Jakob number;
$p$, static pressure in the liquid [dyn/cm²];
$p'$, sum of all normal stresses in the liquid [dyn/cm²];
$p_R$, static pressure at the bubble surface [dyn/cm²];
$p_v$, vapor pressure at temperature $T$ [dyn/cm²];
$p_\infty$, initial uniform static pressure or pressure of the undisturbed liquid at infinite distance from the bubble [dyn/cm²];
$R$, radius of the bubble [cm];
$R_0$, radius of the spherical bubble at the beginning of expansion [cm];
$R'_0$, radius of the cylindrical vapor jet [cm];
$\dot{R}$, velocity of the bubble surface [cm/s];
$\ddot{R}$, acceleration of the bubble surface [cm/s²];
$r$, radius of the considered liquid layer [cm];
$T$, temperature of the bubble [°K];
$T_0$, uniform initial temperature or temperature of the undisturbed liquid at infinite distance from the bubble [°K];
$T_S$, saturation temperature of the vapor corresponding to the pressure $p_\infty$ [°K];
$T_w$, wall temperature [°K];
$t$, time [s];
$t_{99\%}$, time required to reach a value of $R$ equal to 99 per cent of the asymptotic solution prediction [s];
$u$, radial velocity of the liquid [cm/s];
$\theta$, $= T$ [°K];
$\mu$, dynamic viscosity of the liquid [g/cm s];
$\rho$, density of the liquid [g/cm³];
$\rho_v$, density of the vapor [g/cm³];
$\sigma$, surface tension between liquid and its vapor [dyn/cm];
$\tau$, $= t$ [s];
$y$, $= \dot{R} = \dfrac{dR}{dt}$ [cm/s];
$\phi$, $= \dfrac{R}{N'_{Ja}\sqrt{\left(\dfrac{12}{\pi}Dt\right)}}$.

*This paper has been performed within the framework of the association Euratom-Gesellschaft für Kernforschung mbH in the field of fast breeder development.

†Euratom, delegated to the Karlsruhe "Fast Breeder Project", Institut für Neutronenphysik und Reaktortechnik.

## 1. INTRODUCTION

A LIQUID starts to boil when vapor bubbles are allowed to grow from small nuclei in the liquid. These nuclei are essentially very small bubbles of gas or vapor which are contained in microcavities present on the surface of the solid container or produced in the mass of the liquid by any nucleation process, for instance ionisation.

The rate of growth is determined by the inertia of the liquid, by the difference between the pressure within the bubble and the liquid pressure, which of course depends upon the vapor pressure and the surface tension at the bubble boundary, and from the rate at which the liquid can evaporate, i.e. from the rate at which the heat, required by the process of vaporization, can move by conduction from the outer layers of the liquid towards the vapor bubble.

This problem of fundamental importance for the theory of bubble chambers has been widely studied [1–4]. Plesset and Zwick [5, 6] and Foster and Zuber [7] obtained in 1954 two almost identical solutions for the asymptotic period of growth in which inertial and surface tension terms are no longer important and the bubble growth is controlled only by the rates of heat transfer to the moving vapor–liquid interface. These asymptotic solutions are valid only in the case where the thermal boundary-layer thickness at the bubble wall is small in comparison with the bubble radius, that is for relatively high Jakob numbers. Plesset and Zwick gave an analytical solution for the initial period as well [8]. Birkhoff, Margulies and Horning obtained an asymptotic solution without making the restricting assumption on the thickness of the thermal boundary layer, i.e. a solution valid for very small Jakob numbers as well [9]. Almost at the same time Scriven found a similar solution [10]. Bankoff extended the Plesset–Zwick asymptotic solution to not-uniform temperature fields in the liquid [11]. Dergarabedian confirmed the Plesset–Zwick solution by measuring the rate of growth of vapor and air bubbles in slightly superheated water [12].

Papers [5–12] either consider the asymptotic solution or are based on the assumption clearly formulated by Plesset and Zwick [6] that the difference between the undisturbed liquid temperature and the temperature within the bubble, generally indicated as liquid "superheat", is always small, so that the physical properties of liquid and vapor during the process can be considered constant and the pressure differences on the saturation line can be considered proportional to temperature differences. This is legitimate for water at pressures equal to or above atmospheric where those differences are indeed small, but it is not for sodium or other alkali metals, where very high liquid superheats may be present. Experiments with potassium and sodium have shown that, at atmospheric pressure and in presence of normally smooth steel surfaces, liquid superheats as high as 100–200 C are possible, while in extreme cases superheats up to 800 °C have been measured [13–17]. On the other hand the degree of maximum superheat possible in the sodium coolant of a liquid metal fast reactor has a strong influence on the time required by the bubble to reach a diameter equal to that of the coolant subchannels between the fuel pins, both in the case of one single sodium vapor bubble assumed by Schlechtendahl [18] or of a variable number of bubbles assumed by Judd [19] and therefore on the nature and the course of the accident. In effect the Plesset–Zwick asymptotic equation does not apply to sodium in presence of large superheats, although this equation is used by Judd [19], while Schlechtendahl avoids the problem in that he starts to consider the bubble growth when the bubble already has dimensions comparable to those of the cooling channel and the further growth of the bubble depends mainly on the hydraulic resistance of the moving liquid column.

Cole and Shulman [20] show that the Plesset–Zwick asymptotic solution fails to agree with experiment for high Jakob numbers, i.e. essentially for high degrees of superheat. For a Jakob number of 792 corresponding to water boiling at 50 mmHg with a superheat of 20·5 °C the rate of bubble growth is almost an order of magnitude less than that predicted by Plesset–Zwick. Hooper and Abdelmessih [21] report essentially the same conclusions. They find good agreement between their experiments with water at atmospheric pressure and the Plesset–Zwick asymptotic solution for small degrees of superheat (6·8 °C), but considerably smaller rates of growth than those predicted by the theory for larger degrees of superheat (38·8 °C). Another possible limitation to the validity of the Plesset–Zwick equation for sodium is the fact that the coefficient of heat diffusivity in liquid sodium is much higher than that of more common liquids. The role played by the liquid inertia and by the surface tension could be considerable for a relatively longer time, while for a liquid of low heat diffusion (low thermal conductivity), contrary to sodium, the conduction of heat in the liquid around the bubble, and therefore the rate at which the heat of vaporisation is given to the bubble, plays from the outset a dominant role, as in this case it is by far the slowest process.

For the reason discussed above we tried to integrate the differential equations governing the growth of a vapor bubble in superheated liquid sodium, taking into account the variations of sodium properties with temperature. Otherwise the assumptions were the same as those of Plesset and Zwick, that is:

(i) Bubble perfectly spheric

(ii) Uniform pressure and temperature inside the vapor bubble
(iii) The vapor is in thermodynamic equilibrium with the liquid at the bubble interface
(iv) The temperature of the liquid is at the beginning of the process uniform
(v) The liquid is incompressible.

We will discuss the implications of these assumptions later. Because it was not possible to integrate the mentioned differential equations analytically, a method was developed to integrate them by numerical computation with a digital computer.

## 2. ORIGIN OF THE BUBBLE

Consider a microcavity in the heating wall which surrounds the superheated liquid sodium. This cavity contains a certain amount of vapor. We assume that the opening of the cavity is circular. The angle $\theta$ that the separation surface between liquid and vapor makes with the heating wall at the moment of detachment of the bubble from the wall depends on the surface tensions between solid, vapor and liquid. Sodium above 300°C wets a wall very well because the impurities are washed away or in solution, and $\theta$ should be equal to or less than 45°. The bubble is therefore at the moment of detachment from the wall almost perfectly spheric if the surrounding liquid sodium temperature is uniform. This problem is treated in more detail in [22].

In a sodium cooled reactor nucleation centers could be produced by radiation as well. In this case the nucleation centers would be in the mass of the sodium and not in the wall. It is perhaps worthwhile here to treat the formation of nucleation centers directly in the liquid sodium mass in detail. The energy necessary to form a bubble is made up by four contributions [1, 2]:

(i) The energy required to vaporize the mass of liquid involved
(ii) The energy necessary to form a surface between vapor and liquid
(iii) The kinetic energy imparted to the liquid by the motion of the vapor wall
(iv) The viscous losses.

In the present treatment we will neglect the last three terms, which are generally small in comparison with the first one. This is particularly true for sodium at low pressure, such as in a fast reactor core, due to the very high latent heat of vaporization $L$.

In case of bubble formation due to radiation nucleation the energy will be supplied by the energy lost by the radiation particle plus the amount of superheat possibly already present in the liquid. Again, we will neglect this second term because it is small in comparison to $L$ in the range of interest (for sodium at 2 atm and a superheat of $\Delta T = 200°C$, we have: $c \times \Delta T = 0{\cdot}312 \times 200 = 62{\cdot}4$ cal/g, while $L = 884$ cal/g; $c$ is the specific heat of liquid sodium at the saturation temperature corresponding to 2 atm. The sodium physical properties are from [23]). Thus if a radiation particle loses the energy $e$ per unit of track, a cylindrical bubble of vapor will be formed and the radius $R_0'$ of such cylinder is given by:

$$e = \pi R_0'^2 \rho_v L \tag{1}$$

where $\rho_v$ is the density of the sodium vapor.

The well known stability condition for vapor jets in liquid says: "a vapor jet in a liquid breaks up into discrete regions of length comparable to the circumference of the jet" [24]. Thus the cylinder of radius $R_0'$ will break up in spheres of radius $R_0$, the relationship between $R_0'$ and $R_0$ being:

$$\pi R_0'^2 \cdot 2\pi R_0' = \tfrac{4}{3}\pi R_0^3. \tag{2}$$

From (1) and (2) one obtains:

$$R_0 = \sqrt{\left[\frac{(3\pi/2)^{2/3}}{\pi}\frac{e}{\rho_v L}\right]}. \tag{3}$$

The radiation field in sodium in a fast core consists of $\beta, \gamma$ and neutron radiation. The $\beta$-radiation is due to the $\beta$-decay of $Na^{24}$. Since $\gamma$ quanta are only efficient when they are converted into electrons we have to consider the stopping of electrons and of sodium ions formed by collisions with fast neutrons only.

The energy release in slowing down of electrons in matter is a very complex phenomenon, but for our purpose a rough estimate of the energy loss is sufficient. For the average energy decrease of 1·4 MeV electrons in very thin layers of aluminium the experimental value is [25]

$$e = 1{\cdot}2\,\text{keV/mg cm}^{-2}$$

in good agreement with theory. Since the atomic number and charge of sodium are similar to those of aluminium we can assume that this value also roughly holds for sodium. If we further assume that the total energy is transferred into heat we have with $\rho = 0{\cdot}72$ g/cm$^3$*

$$e = 0{\cdot}87\,\text{MeV/cm} = 3{\cdot}3 \times 10^{-14}\,\text{cal/cm}.$$

If a 2 MeV neutron collides with a sodium atom a recoil ion of about 160 keV is formed. The information concerning the energy loss of ions heavier than $\alpha$ particles is very fragmentary [26] but from a reasonable

*$\rho$ is the density of liquid sodium at the saturation point at 2 atm.

extrapolation of existing data one gets at least the order of magnitude which is

$$\frac{1}{N}e = 5\times 10^{-14}\,\text{eV cm}^2/\text{atom}$$

or with

$$N_{Na} = 1{\cdot}88\times 10^{22}/\text{cm}^3$$

$$e = 940\,\text{MeV/cm} = 3{\cdot}57\times 10^{-11}\,\text{cal/cm}.$$

This value is almost three orders of magnitude higher than the one for the electrons but still very low. Much higher energy densities would be obtained, however, if fission products would be released directly into the sodium. Then about 60 MeV would be absorbed in a distance of 2·8 mg/cm$^2$ of aluminium [27]. If we again assume this value to be the same for sodium we get

$$e = 1{\cdot}54\times 10^{4}\,\text{MeV/cm} = 5{\cdot}9\times 10^{-10}\,\text{cal/cm}.$$

Our conclusions are little affected by the choice of sodium pressure in the range interesting for fast reactors (1–10 atm). However, we take as typical of sodium in a fast core, sodium at 2 atm. In this condition $L = 884$ cal/g and $\rho_v$ (density of sodium saturated vapor at 2 atm) is $0{\cdot}557\times 10^{-3}$ g/cm$^3$. Equation (3) becomes:

$$R_0 = \sqrt{(1{\cdot}82\,e)} \tag{4}$$

where $e$ is in cal/cm and $R_0$ in cm.

Using for $e$ the values obtained above, one has respectively for electrons, fast neutrons and fission products, bubbles of radii: 0·0025, 0·08 and 0·33 $\mu$. In [22] it is shown that, with normal smooth stainless steel surfaces in presence of liquid metals, the biggest surface cavities still active, i.e. still full of vapor or gas after a long time in contact with the liquid and not filled up by the liquid itself, have an opening radius of about 0·25 $\mu$. This corresponds to a maximum possible sodium superheat of 204°C at 2 atm. That is, only when the sodium at the wall is superheated by that amount can the vapor bubbles in the wall grow. Therefore all the radiation bubbles of radius less than 0·25 $\mu$ require higher liquid superheats to grow, or, conversely, they do not reduce the maximum possible sodium superheat given by a normal smooth stainless steel surface.

It seems therefore unlikely that any of the nuclear radiations present in sodium in a fast reactor core will induce nucleation of vapor bubbles in the bulk of liquid sodium before boiling occurs at surface cavities. Only if fission products were generated directly in contact with sodium would the superheat required by the bubble to grow be of the same order of magnitude as that required by the cavities present in normal smooth stainless steel surfaces. Claston reaches more or less the same conclusion with a more detailed analysis [28].

## 3. THE DIFFERENTIAL EQUATIONS

### 3.1. *Equation of motion*

The equation of motion of a viscous incompressible fluid (Navier–Stokes's equation) in spherical coordinates is in presence of a spherical symmetry (see [29] p. 109):

$$\frac{\partial u}{\partial t}+u\frac{\partial u}{\partial r} = -\frac{1}{\rho}\frac{\partial p'}{\partial r}+\frac{\mu}{\rho}\left[\frac{1}{r^2}\frac{\partial}{\partial r}\left(r^2\frac{\partial u}{\partial r}\right)-\frac{2u}{r^2}\right]. \tag{5}$$

While the equation of continuity is (incompressible liquid: $\rho = \text{const.}$):

$$\frac{\partial}{\partial r}(r^2u) = 0. \tag{6}$$

From equation (6) it follows:

$$\frac{\partial u}{\partial r} = -2\frac{u}{r} \tag{7}$$

and

$$\frac{\partial}{\partial r}\left(r^2\frac{\partial u}{\partial r}\right) = \frac{\partial}{\partial r}(-2ur) = 2u. \tag{8}$$

The last term of equation (5) is therefore equal to zero. This is to be expected because no tangential stresses are present due to the spherical symmetry. Equation (5) becomes:

$$\frac{\partial u}{\partial t}-2\frac{u^2}{r} = -\frac{1}{\rho}\frac{\partial p'}{\partial r}. \tag{9}$$

Where $p'$ is the sum of all the normal stresses and it is given by the static pressure plus the normal friction stresses:

$$p' = p+2\mu\frac{\partial u}{\partial r} = p-4\mu\frac{u}{r}. \tag{10}$$

The factor 2 is given by the two angular directions normal to $r$ {see equation (17) on p. 95 of [29]}.

Replacing (10) in (9) and observing that

$$\frac{\partial}{\partial r}\left(\frac{u}{r}\right) = -\frac{3u}{r^2} \tag{11}$$

we obtain:

$$\frac{\partial u}{\partial t}-\frac{2u^2}{r} = -\frac{1}{\rho}\frac{\partial p}{\partial r}-12\frac{\mu}{\rho}\frac{u}{r^2}. \tag{12}$$

If $R$ is the radius of the expanding vapor bubble at the time $t$, the equation of continuity requires:

$$u = \frac{R^2\dot{R}}{r^2} \tag{13}$$

thus

$$\frac{\partial u}{\partial t} = \frac{\ddot{R}R^2+2R\dot{R}^2}{r^2} \tag{14}$$

and equation (12) becomes:

$$\frac{\ddot{R}R^2+2R\dot{R}^2}{r^2}-2\frac{R^4\dot{R}^2}{r^5} = -\frac{1}{\rho}\frac{\partial p}{\partial r}-12\frac{\mu}{\rho}\frac{R^2\dot{R}}{r^4}. \tag{15}$$

By integrating equation (15) between $r$ and $r = \infty$ with the assumption that that $\mu$ and $\rho$ are constant in the region of the liquid, one obtains:

$$\frac{\ddot{R}R^2+2R\dot{R}^2}{r}-\frac{\dot{R}^2R^4}{2r^4}+4\frac{\mu}{\rho}\frac{R^2\dot{R}}{r^3}=\frac{p-p_\infty}{\rho}. \quad (16)$$

For $r = R$ equation (16) becomes:

$$\ddot{R}R+\tfrac{3}{2}\dot{R}^2+4\frac{\mu\dot{R}}{\rho R}=\frac{p_R-p_\infty}{\rho}. \quad (17)$$

The pressure $p_R$ of the liquid at the bubble boundary is given in terms of the vapor pressure $p_v(T)$ within the bubble by:

$$p_R = p_v(T)-\frac{2\sigma(T)}{R} \quad (18)$$

where $\sigma(T)$ is the surface tension between vapor and liquid and $p_v(T)$ is the equilibrium vapor pressure for the temperature $T$ at the bubble boundary.

The initial conditions are:

$$R(o) = R_0; \quad \dot{R}(o) = 0; \quad T(r, o) = T_0 \quad (19)$$

$R_0$ is the effective initial radius of the bubble, which is at the beginning in unstable equilibrium and surrounded by superheated liquid at the uniform temperature $T_0$ and uniform pressure $p_\infty$.

From equations (17), (18), (19) one has:

$$p_\infty = p_R(o) = p_v(T_0)-\frac{2\sigma(T_0)}{R_0} \quad (20)$$

and replacing (18) and (20) in (17):

$$\ddot{R} = \frac{2[\sigma(T_0)R-\sigma(T)R_0]}{\rho R_0 R^2}-\tfrac{3}{2}\frac{\dot{R}^2}{R} -\frac{p_v(T_0)-p_v(T)}{\rho R}-4\frac{\mu}{\rho}\frac{\dot{R}}{R^2}. \quad (21)$$

The first term on the left side of this equation represents the effect of the surface tension, the second the inertia of the liquid, the third the cooling effect due to evaporation and the fourth the effect of the viscous forces. This equation without the last two terms was obtained originally by Lord Rayleigh [30], while the third term on the left side of equation (21) was introduced by Plesset and Zwick [6]. The Lord Rayleigh solution would of course give too high values of $R$ and therefore too high expansion rates of the bubble. As Plesset and Zwick already noticed in their paper the cooling effect reduces considerably the expansion velocity of the bubble for water with relatively low initial degrees of superheat. We will see that this is also the case for sodium even in presence of high values of liquid superheat. However, for sodium, the effect of the viscosity forces is, apart from the very initial phase, practically negligible.

### 3.2. *Energy equation*

The energy equation in spherical coordinates in presence of spherical symmetry is given by:

$$\frac{\partial T}{\partial r}+u\frac{\partial T}{\partial r}=D\left(\frac{\partial^2 T}{\partial r^2}+\frac{2}{r}\frac{\partial T}{\partial r}\right)+\frac{b}{\rho c} \quad (22)$$

and considering equation (13):

$$\frac{\partial T}{\partial r}+\frac{R^2\dot{R}}{r^2}\frac{\partial T}{\partial r}=D\left(\frac{\partial^2 T}{\partial r^2}+\frac{2}{r}\frac{\partial T}{\partial r}\right)+\frac{b}{\rho c} \quad (23)$$

where $D$ is the thermal diffusivity in the liquid and $b$ the heat produced in the liquid for unit volume and time.

The energy required by the expansion of the bubble is transmitted by conduction in the superheated liquid to the bubble. Thus at the bubble boundary one has:

$$4\pi R^2 k\left(\frac{\partial T}{\partial r}\right)_{r=R}=\frac{\mathrm{d}}{\mathrm{d}t}\left[\tfrac{4}{3}\pi R^3 L\rho_v+\frac{4\pi R^2\sigma}{J} +\tfrac{4}{3}\pi R^3\frac{(p_R-p_v)}{J}\right]. \quad (24)$$

The first term on the left side of equation (24) represents the heat coming by conduction through the liquid, the first term on the right side is the heat required by the evaporation of the liquid, the second the energy of the surface (transformed into heat units by the conversion factor $J$) and the third the work done in creating a spherical hole of radius $R$ against a liquid pressure $p_R$ minus the work in filling it with vapor at the pressure $p_v$. The surface energy of the bubble and the work against the pressure are small in comparison with the evaporation heat of the bubble, but not always negligible, thus we considered them in the calculations. The numerical calculations showed, however, that for sodium and water the terms relative to the kinetic energy imparted to the liquid by the motion of the vapor wall:

$$\frac{1}{J}\frac{\mathrm{d}}{\mathrm{d}t}[2\pi\rho R^3\dot{R}^2]$$

and the heat dissipated by the viscous losses:

$$\frac{16\pi}{J}\mu R\dot{R}^2$$

are always negligible in comparison with the other terms. Taking into account equation (18), equation (24) can be written in the form:

$$\left(\frac{\partial T}{\partial r}\right)_{r=R}=\frac{L\rho_v\dot{R}}{k}+\tfrac{2}{3}\frac{\sigma}{Jk}\frac{\dot{R}}{R} +\left[\frac{R}{3k}\frac{\partial(L\rho_v)}{\partial T}+\frac{1}{3Jk}\frac{\partial\sigma}{\partial T}\right]\left[\dot{R}\left(\frac{\partial T}{\partial r}\right)_{r=R}+\left(\frac{\partial T}{\partial t}\right)_{r=R}\right]. \quad (25)$$

A further boundary condition for the temperature [besides the initial condition contained in equation (19)] is given by:

$$T(\infty, t) = T_0 + \frac{b}{\rho c} t. \tag{26}$$

The term $b/\rho c$ is necessary to allow the expansion of the bubble from the initial position of unstable equilibrium [see equations (19) and (21)]. In the present calculations we have used values typical for a sodium cooled fast reactor core; however, unless extremely high and unrealistic values are assumed, this parameter does not affect the subsequent growth rate of the bubble.

## 4. MATHEMATICAL TREATMENT AND NUMERICAL SOLUTION

We have to solve: (a) the equation of motion of the bubble (21) for $R$ where $\rho$, $\sigma$, $\mu$ and $p_v$ are functions of $T$, and (b) the equation of heat conduction in the liquid (23) for $T$ where $D$, $\rho$ and $c$ are functions of $T$, under the initial conditions of equations (19) and the boundary conditions given by equations (25) and (26), where again $\rho$, $c$, $L\rho_v$, $k$ and $\sigma$ are functions of $T$. The initial temperature $T_0$ is given by equation (20) where $p_\infty$ and $R_0$ are known.

As the equations (21) and (23) are not independent of each other, we proceed as follows: we start by putting into equation (21) values of $\rho$, $\sigma$ and $\mu$ at the temperature $T_1$ given by:

$$T_1 = T_0 + \frac{b}{\rho(T_0)c(T_0)} \Delta t. \tag{27}$$

This temperature $T_1$ may be considered constant during the time interval $\Delta t$, sufficiently small. Then we solve the equation (21) for $R$ and $\mathrm{d}R/\mathrm{d}t$ at $t_1 = 0 + \Delta t$ under the given initial conditions $R(o) = R_0$ and $\mathrm{d}R/\mathrm{d}t = 0$. With those values $R_1$ and $\mathrm{d}R_1/\mathrm{d}t$, the physical properties evaluated at $T_1$, and

$$\frac{\partial T}{\partial t} = \frac{T_1 - T_0}{\Delta t} = \frac{b}{\rho(T_0)c(T_0)} \tag{28}$$

we calculate from equations (23) and (25) the temperature distribution in the liquid surrounding the bubble at the time $t_1$. From this temperature distribution we obtain for $r = R(t_1)$ a new value of $T_1$, which we use in equation (21) to obtain better values of $R_1$ and $\mathrm{d}R_1/\mathrm{d}t$ at the time $t_1$. This procedure is iterated until the relative variation of $\mathrm{d}R/\mathrm{d}t$ from one iteration to the following is sufficiently small. Then we repeat this process for the next time $t_2 = t_1 + \Delta t$ with initial temperature $T_1$ constant in the time interval $t_2 - t_1$ and the initial values $R_1$ and $\mathrm{d}R_1/\mathrm{d}t$. We continue with the following time intervals until the asymptotic temperature is reached.

In practice to do so we have to transform equations (21), (23), (25). The differential equation of second order (21) is replaced by the system of two differential equations of the first order:

$$\begin{cases} \dfrac{\mathrm{d}R}{\mathrm{d}t} = y \\ \dfrac{\mathrm{d}y}{\mathrm{d}t} = \dfrac{2[\sigma(T_0)R - \sigma(T)R_0]}{\rho(T)R_0 R^2} - \dfrac{3}{2}\dfrac{y^2}{R} - \dfrac{p_v(T_0) - p_v(T)}{\rho(T)R} - 4\dfrac{\mu(T)}{\rho(T)}\dfrac{y}{R^2}. \end{cases} \tag{29}$$

We have solved this system with the Runge–Kutta method of the SSP-IBM library. The time step must initially be of the order of $10^{-8}$ s and we increase it as the radius grows. The time at which the asymptotic temperature is reached depends on the initial value of the radius of the bubble $R_0$ and on the initial liquid pressure $p_\infty$, and lies between $10^{-2}$ s and a few seconds.

The equation (23), a partial differential equation of the parabolic type with boundary conditions, can be solved for small space steps. As the radius $R$ of the bubble increases with the time (we start with values of $R_0$ in the range $2{\cdot}5 \times 10^{-5}$ cm to $10^{-3}$ cm, and we calculate values of $R$ in the order of 10 cm) we must change the space step in the liquid. It is generally in our calculations taken equal to $R/100$. From one time step to the next, we obtain the initial temperature distribution on the new mesh points by interpolation and extrapolation from the values of the preceding time step.

A convenient method to choose the grid and obtain a system of finite difference grid equations, which permits an optimal transcription of our boundary value problem, is suggested by Babuska *et al.* [31]. To use this method we introduce a transformation to the Lagrange coordinates $h$, $\tau$ with the position:

$$\begin{cases} h = \frac{1}{3}[r^3 - R^3(t)] \\ \tau = t \\ \theta(h, \tau) = T(r, t). \end{cases} \tag{30}$$

Hence:

$$\begin{aligned} &\frac{\partial h}{\partial r} = r^2 \qquad \frac{\partial h}{\partial t} = -R^2(t)\dot{R} \\ &\frac{\partial \tau}{\partial r} = 0 \qquad \frac{\partial \tau}{\partial t} = 1 \end{aligned} \tag{31}$$

and:

$$\begin{aligned} &\frac{\partial T}{\partial r} = \frac{\partial \theta}{\partial h}\frac{\partial h}{\partial r} + \frac{\partial \theta}{\partial \tau}\frac{\partial \tau}{\partial r} = r^2 \frac{\partial \theta}{\partial h} \\ &\frac{\partial^2 T}{\partial r^2} = \frac{\partial}{\partial r}\left(r^2 \frac{\partial \theta}{\partial h}\right) = 2r\frac{\partial \theta}{\partial h} + r^4 \frac{\partial^2 \theta}{\partial h^2} \\ &\frac{\partial T}{\partial t} = \frac{\partial \theta}{\partial h}\frac{\partial h}{\partial t} + \frac{\partial \theta}{\partial \tau}\frac{\partial \tau}{\partial t} = -R^2\dot{R}\frac{\partial \theta}{\partial h} + \frac{\partial \theta}{\partial \tau}. \end{aligned} \tag{32}$$

Substituting equations (30), (31), (32) in equation (23) we obtain:

$$\frac{\partial\theta}{\partial\tau} = D(\theta)\frac{\partial}{\partial h}\left[[3h+R^3(\tau)]^{4/3}\frac{\partial\theta}{\partial h}\right] + \frac{b}{\rho(\theta)c_p(\theta)} \quad (33)$$

while the boundary conditions may be obtained by substituting equations (30), (31), (32) in equations (19), (25), (26):

$$\theta(h,0) = T_0 \quad (34)$$

$$R^2(\tau)\frac{\partial\theta(0,\tau)}{\partial h} = \frac{L(\theta(0,\tau))\cdot\rho_v(\theta(0,\tau))}{k(\theta(0,\tau))}\dot{R}(\tau) + \frac{2\sigma(\theta(0,\tau))}{3Jk(\theta(0,\tau))}\frac{\dot{R}(\tau)}{R(\tau)} + \left\{\frac{R(\tau)}{3k(\theta(0,\tau))}\frac{\partial[L(\theta(0,\tau))\cdot\rho_v(\theta(0,\tau))]}{\partial\theta} + \frac{1}{3Jk(\theta(0,\tau))}\frac{\partial\sigma(\theta(0,\tau))}{\partial\theta}\right\}\frac{\partial\theta(0,\tau)}{\partial\tau} \quad (35)$$

$$\theta(\infty,t) = T_0 + \frac{b}{\rho(\theta)c(\theta)}t. \quad (36)$$

We cover the integration field with a rectangular grid with the mesh points:

$$x_K = K\cdot\Delta h \qquad K = 0,1,\ldots,n$$
$$\tau_l = l\cdot\Delta\tau \qquad l = 1,\ldots,m. \quad (37)$$

For the coefficients of (33) and (35) we assume:

$$D(\theta_l) = \frac{k(\bar{\theta}_{l-1})}{\rho(\bar{\theta}_{l-1})\cdot c(\bar{\theta}_{l-1})} \quad (38)$$

$$\frac{b}{\rho(\bar{\theta}_l)\cdot c(\bar{\theta}_l)} = \frac{b}{\rho(\bar{\theta}_{l-1})\cdot c(\bar{\theta}_{l-1})} \quad (39)$$

constant in a time interval $\Delta\tau$ and calculated for an average temperature

$$\bar{\theta}_{l-1} = \frac{\theta(x_0,\tau_{l-1})+\theta(x_n,\tau_{l-1})}{2}. \quad (40)$$

We assume furthermore that:

$$\frac{L(\theta(0,\tau_l))\cdot\rho_v(\theta(0,\tau_l))}{k(\theta(0,\tau_l))} = A'_{l-1} + B'_{l-1}\theta(0,\tau_l) \quad (41)$$

$$\frac{2\sigma(\theta(0,\tau))}{3Jk(\theta(0,\tau))} = A'' + B''\theta(0,\tau_l) \quad (42)$$

are linear functions of $\theta(0,\tau_l)$ and

$$\frac{1}{3k(\theta(0,\tau))}\frac{\partial[L(\theta(0,\tau))\cdot\rho_v(\theta(0,\tau))]}{\partial\theta} = B_{l-1} \quad (43)$$

$$\frac{1}{3Jk(\theta(0,\tau))}\frac{\partial\sigma(\theta(0,\tau))}{\partial\theta} = \frac{A''}{k(\theta(0,\tau_{l-1}))} = C_{l-1} \quad (44)$$

are constant in the time interval $\Delta\tau$.

The parameters $B_{l-1}$, $C_{l-1}$, $A'_{l-1}$, $B'_{l-1}$ assumed constant in the time interval $\Delta\tau$ are calculated for the temperature $\theta(0,\tau_{l-1})$. Appendix 1 shows how they and the constants $A''$, $A'''$, $B''$ can be calculated from the physical properties of sodium or water. We can now write the system of grid equations for equations (33) and (35) using the method suggested by Babuska *et al.* [31] where we choose for the convergence parameter $\alpha$ the value $\alpha = \frac{1}{2}$ to be free from any restrictions on the magnitude of the space and time steps. The (33) becomes:

$$-\frac{1}{2\Delta h}(3x_{k-1/2}+R^3(\tau_l))^{4/3}\cdot\theta(x_{k-1},\tau_l) + \left\{\frac{1}{2\Delta h}[(3x_{k+1/2}+R^3(\tau_l))^{4/3} + (3x_{k-1/2}+R^3(\tau_l))^{4/3}] + \frac{\Delta h}{D_{l-1}\Delta\tau}\right\}\theta(x_k,\tau_l) - \frac{1}{2\Delta h}(3x_{k+1/2}+R^3(\tau_l))^{4/3}\cdot\theta(x_{k+1},\tau_l) = \frac{1}{2\Delta h}[(3x_{k-1/2}+R^3(\tau_{l-1}))^{4/3}]\cdot\theta(x_{k-1},\tau_{l-1}) + \left\{-\frac{1}{2\Delta h}[(3x_{k-1/2}+R^3(\tau_{l-1}))^{4/3} + (3x_{k+1/2}+R^3(\tau_{l-1}))^{4/3}] + \frac{\Delta h}{D_{l-1}\Delta\tau}\right\}\theta(x_k,\tau_{l-1}) + \frac{1}{2\Delta h}(3x_{k+1/2}+R^3(\tau_{l-1}))^{4/3}\theta(x_{k+1},\tau_{l-1}) + \frac{\Delta h}{2k_{l-1}}(b(\tau_l)-b(\tau_{l-1})) \quad (45)$$

for $k = 1,2,\ldots n-1$.

The boundary condition (35) becomes:

$$\left\{\frac{1}{2\Delta h}(3x_{1/2}+R^3(\tau_l))^{4/3} + \frac{\Delta h}{2D_{l-1}\Delta\tau} + \frac{\dot{R}(\tau_l)}{2}(B'_{l-1}R^2(\tau_l)+B''R(\tau_l)) + \frac{1}{2\Delta\tau}[B_{l-1}R^3(\tau_l)+C_{l-1}R^2(\tau_l)+B_{l-1}R^3(\tau_{l-1}) + C_{l-1}R^2(\tau_{l-1})]\right\}\cdot\theta(0,\tau_l) - \frac{1}{2\Delta h}(3x_{1/2}+R^3(\tau_l))^{4/3}\theta(x_1,\tau_l) = \left\{-\frac{1}{2\Delta h}(3x_{1/2}+R^3(\tau_{l-1}))^{4/3} + \frac{\Delta h}{2D_{l-1}\Delta\tau} - \frac{\dot{R}(\tau_{l-1})}{2}(B'_{l-1}R^2(\tau_{l-1})+B''R(\tau_{l-1})) + \frac{1}{2\Delta\tau}[B_{l-1}R^3(\tau_l)+C_{l-1}R^2(\tau_l)+B_{l-1}R^3(\tau_{l-1}) + C_{l-1}R^2(\tau_{l-1})]\right\}\theta(0,\tau_{l-1}) + \frac{1}{2\Delta h}\cdot(3x_{1/2}+R^3(\tau_{l-1}))^{4/3}\theta(x_1,\tau_{l-1}) + \frac{\Delta h}{4k_{l-1}}(b(\tau_l)+b(\tau_{l-1})) - \tfrac{1}{2}[\dot{R}(\tau_l)R(\tau_l)(A'_{l-1}R(\tau_l)+A'') + \dot{R}(\tau_{l-1})R(\tau_{l-1})(A'R(\tau_{l-1})+A'')] \quad (46)$$

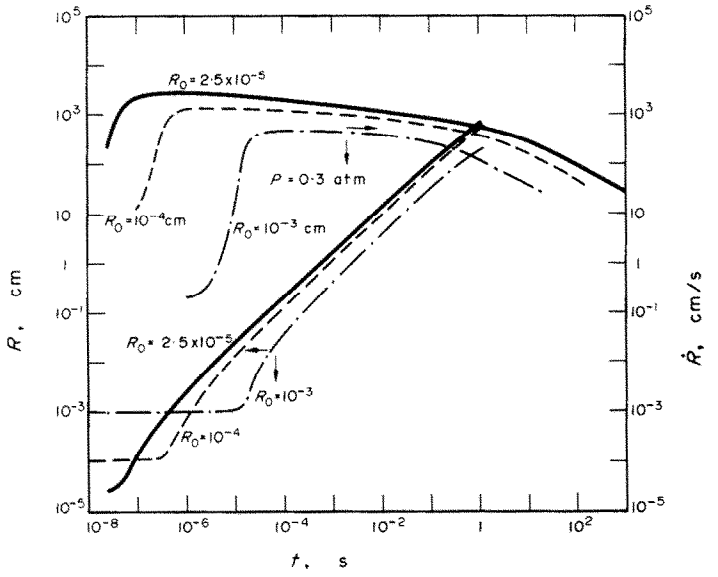


FIG. 1. $R, \dot{R}$ vs $t$ for $p = 0{\cdot}3$ atm, $R_0 = 2{\cdot}5 \times 10^{-5}, 10^{-4}, 10^{-3}$ cm.

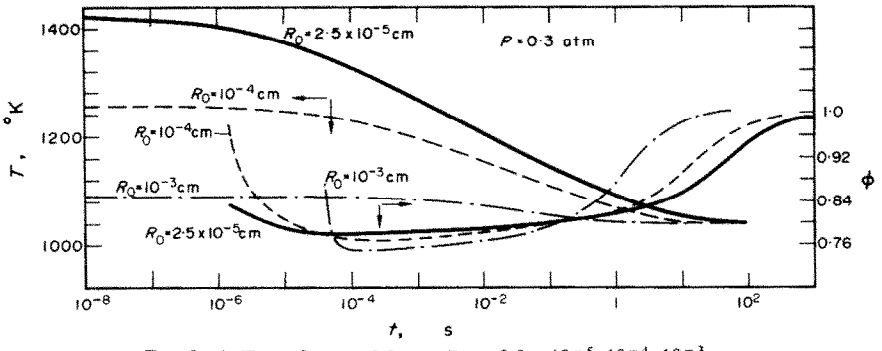


FIG. 2. $\phi$, $T$ vs $t$ for $p = 0{\cdot}3$ atm, $R_0 = 2{\cdot}5 \times 10^{-5}, 10^{-4}, 10^{-3}$ cm.

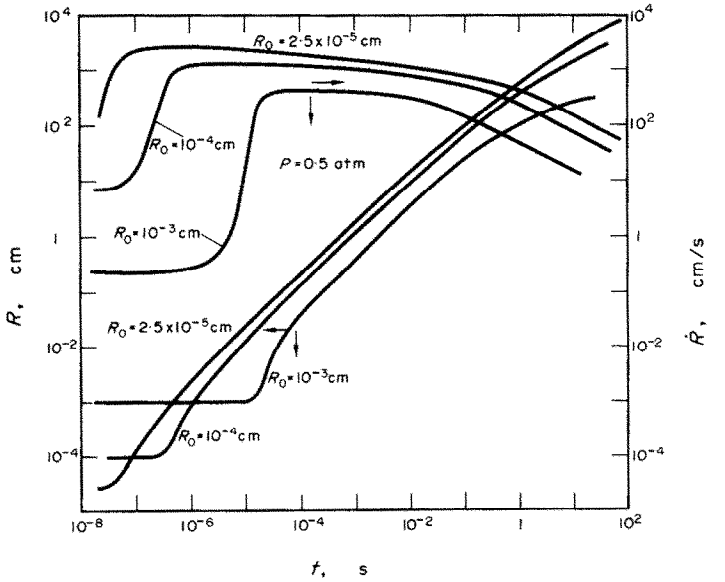


FIG. 3. $R, \dot{R}$ vs $t$ for $p = 0{\cdot}5$ atm, $R_0 = 2{\cdot}5 \times 10^{-5}, 10^{-4}, 10^{-3}$ cm.

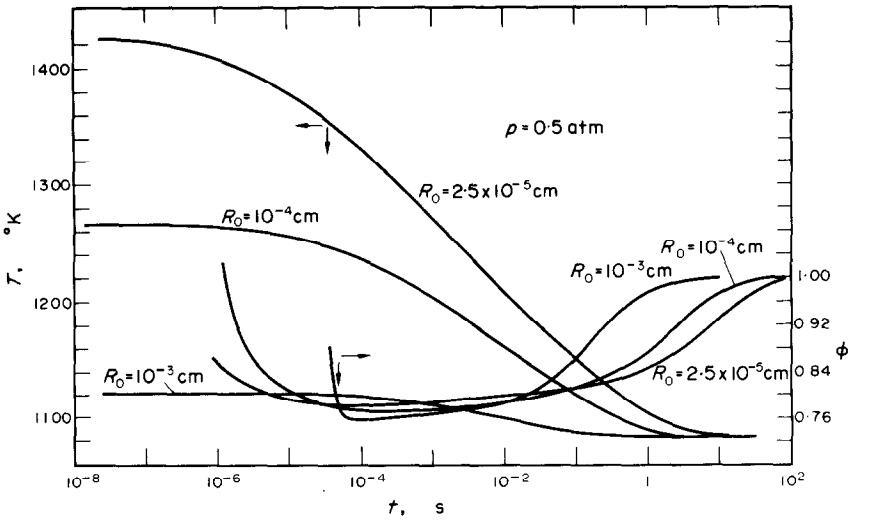


FIG. 4. $\phi$, $T$ vs $t$ for $p = 0{\cdot}5$ atm, $R_0 = 2{\cdot}5 \times 10^{-5}$, $10^{-4}$, $10^{-3}$ cm.

Equations (45) and (46) are written for each $\tau_l$, $l = 1, \ldots, m$. The linear system (45), (46) is tridiagonal and diagonally dominant and can be directly solved [32]. The stability with respect to growth of rounding errors has been shown by Wilkinson [33]. A computer program Hydrodynamic BUBBLE was written for the IBM 370/165 using these equations.

## 5. INTEGRATION RESULTS

Figures 1–14 show the results of the calculations performed with the help of HY-BUBBLE for sodium in a range of pressures related to the core of a sodium cooled reactor ($0{\cdot}3 \leqslant p \leqslant 6$ atm). The initial values $R_0$ of the bubble were chosen between $2{\cdot}5 \times 10^{-5}$ cm and $10^{-3}$ cm giving a range of initial liquid superheats between 5 and 380°C. The figures show the values of $R$, $\dot{R}$, $T$ and $\phi$ at the surface of the expanding bubble vs time. The calculations were generally performed with $bt/\rho c$ of the order of $10^{-2}$°C in equation (26), while in equations (45) and (46) for simplicity $b$ was assumed equal zero. With HY-BUBBLE it is however possible to perform calculations with $b \neq 0$, and with $T_0$ and $p_\infty$ as functions of time.

$\phi$ is the ratio between the calculated value of $R$ and the value of $R$ which would have given by the Plesset–Zwick asymptotic solution with a "transient" Jakob number in place of the usual "asymptotic" Jakob number:

$$\phi = \frac{R}{N'_{Ja}\sqrt{\left(\frac{12}{\pi}Dt\right)}} \tag{47}$$

with

$$N'_{Ja} = \frac{\rho c(T_0 - T)}{\rho_v(T)L(T)}$$

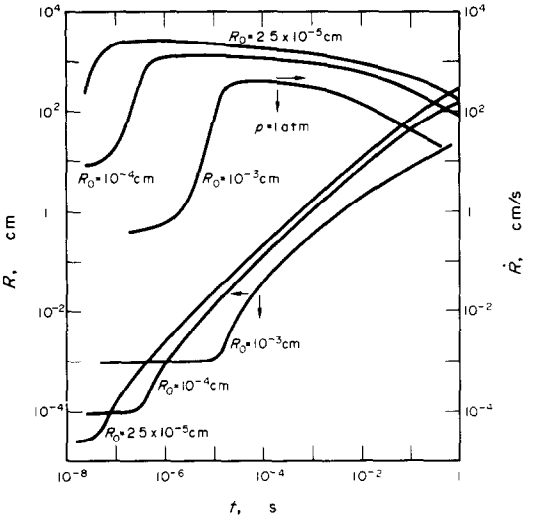


FIG. 5. $R$, $\dot{R}$ vs $t$ for $p = 1$ atm, $R_0 = 2{\cdot}5 \times 10^{-5}$, $10^{-4}$, $10^{-3}$ cm.

while the definition of the Jakob number used in the Plesset–Zwick asymptotic solution is:

$$N_{Ja} = \frac{\rho c(T_0 - T_s)}{\rho_v(T_s)L(T_s)}. \tag{48}$$

The main difference between the two definitions is given by the temperature difference used in the formula. This difference can be considered the "driving force" in the expansion of the bubble when the conduction in the liquid surrounding the bubble plays a dominant role. In the transient Jakob number definition this difference is given by the actual difference between the temperature $T_0$ of the undisturbed liquid and the temperature $T$ at the bubble surface at the considered

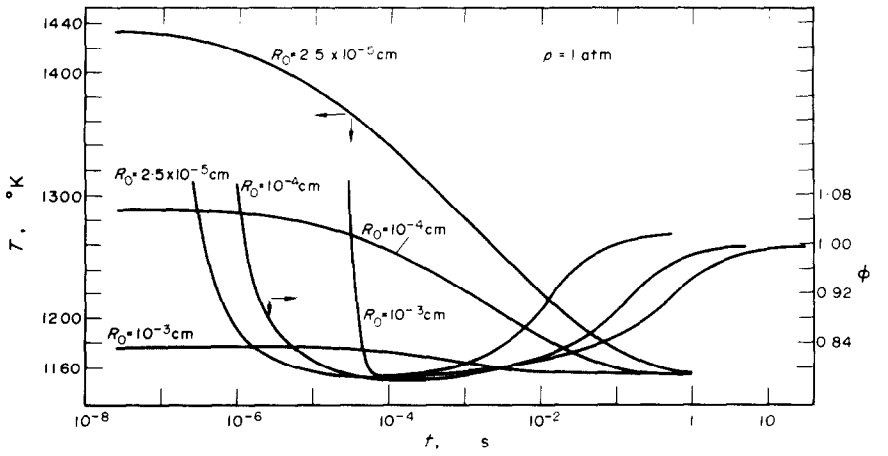


FIG. 6. $\phi$, $T$ vs $t$ for $p = 1$ atm, $R_0 = 2{\cdot}5 \times 10^{-5}, 10^{-4}, 10^{-3}$ cm.

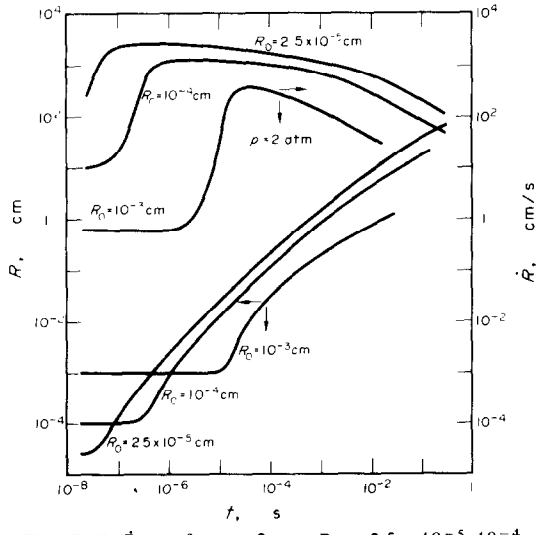


FIG. 7. $R$, $\dot{R}$ vs $t$ for $p = 2$ atm, $R_0 = 2{\cdot}5 \times 10^{-5}, 10^{-4}, 10^{-3}$ cm.

time $t$, assumed constant within the bubble. In the usual definition of the Jakob number $T$ is replaced by $T_s$, saturation temperature corresponding to the liquid pressure because $T$ is generally not known and $T$ tends asymptotically to $T_s$ for $t \to \infty$. From the figures one can see that during the transient $\phi$ never decreases below 0·75. This indicates that even during the transient the most important factor in determining the bubble growth is the heat conduction in the surrounding liquid, the combined effect on $R$ of all the other factors being less than 25 per cent. The growth of a bubble in superheat sodium can be roughly described by the Plesset–Zwick solution provided the Jakob number is replaced by the "transient" Jakob number. This however requires the knowledge of the actual temperature of the bubble during the transient, which is generally not known and requires detailed and complicated calculations of the type we have performed.

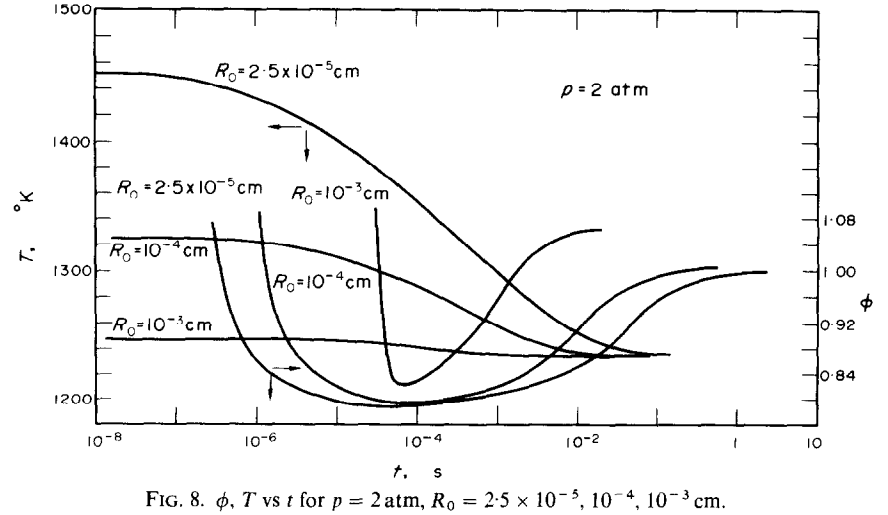


FIG. 8. $\phi$, $T$ vs $t$ for $p = 2$ atm, $R_0 = 2{\cdot}5 \times 10^{-5}, 10^{-4}, 10^{-3}$ cm.

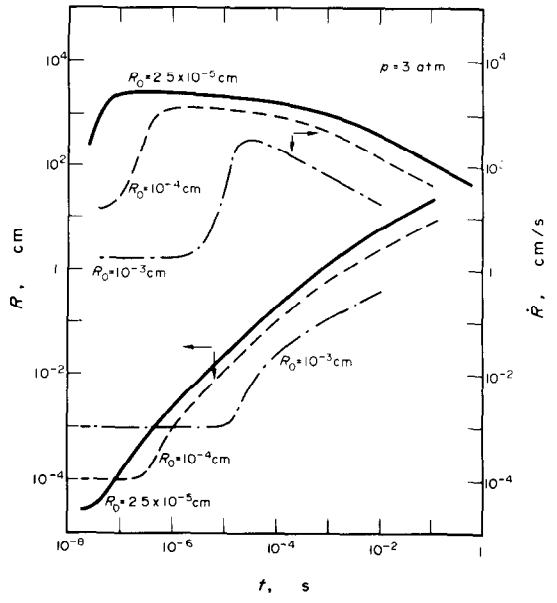


FIG. 9. $R$, $\dot{R}$ vs $t$ for $p = 3$ atm, $R_0 = 2{\cdot}5 \times 10^{-5}$, $10^{-4}$, $10^{-3}$ cm.

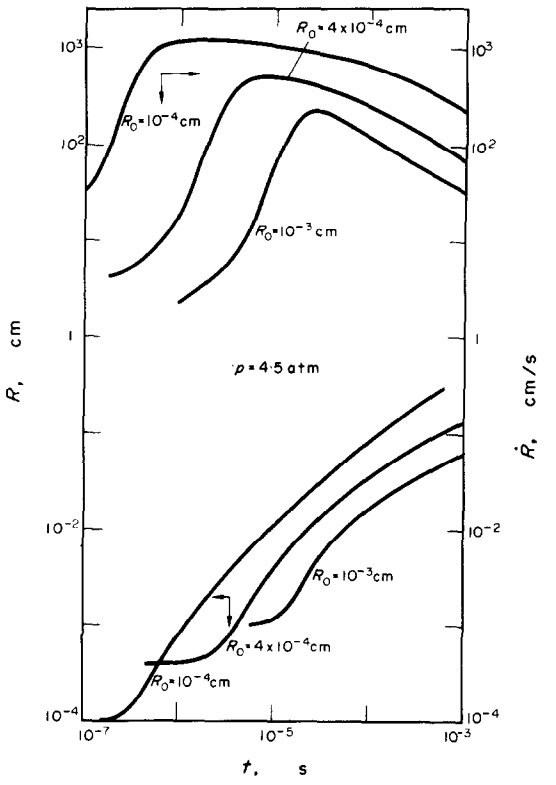


FIG. 11. $R$, $\dot{R}$ vs $t$ for $p = 4{\cdot}5$ atm, $R_0 = 10^{-4}$, $4 \times 10^{-4}$, $10^{-3}$ cm.

Figures 1–14 show that in presence of large degrees of superheat ($T_0 - T_s > 20°$, see also Table 1 to obtain the value of $T_0 - T_s$ for a given pair $p_\infty$, $R_0$) there is a relatively long period of time where $\dot{R}$ remains relatively constant. This fact was correctly assumed by Schlechtendahl [34] to show that the growth of a bubble in sodium suppresses the growth of other nucleation centers in a region surrounding the bubble. This in turn explains why in sodium in presence of large superheats boiling occurs with few large bubbles.

Figure 15 shows the values of $R/\sqrt{(Dt)}$ for $t \to \infty$ vs the asymptotic Jakob number. The agreement between the points calculated with the present numerical approach and the analytical solutions predicted by Plesset and Zwick for high Jakob numbers [6] and by Birkhoff *et al.* for low Jakob numbers [9] is excellent.

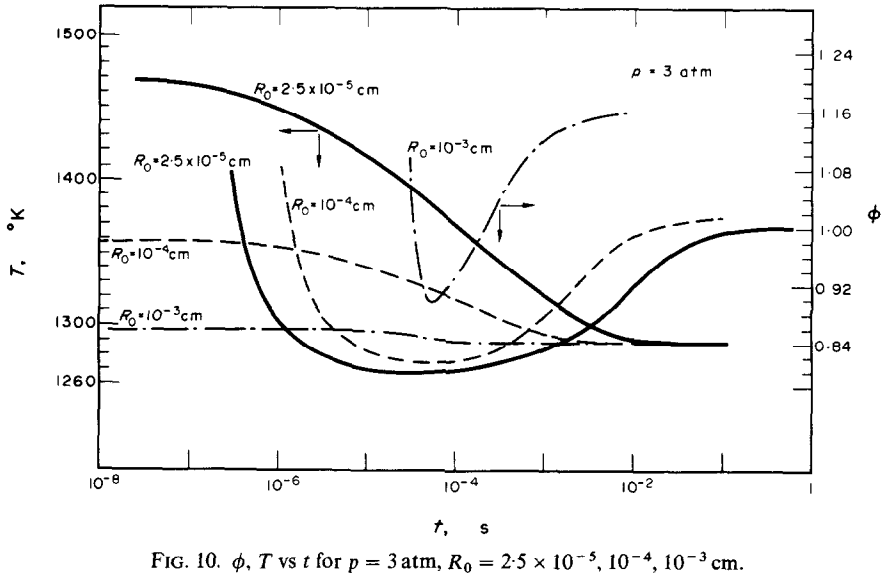


FIG. 10. $\phi$, $T$ vs $t$ for $p = 3$ atm, $R_0 = 2{\cdot}5 \times 10^{-5}$, $10^{-4}$, $10^{-3}$ cm.

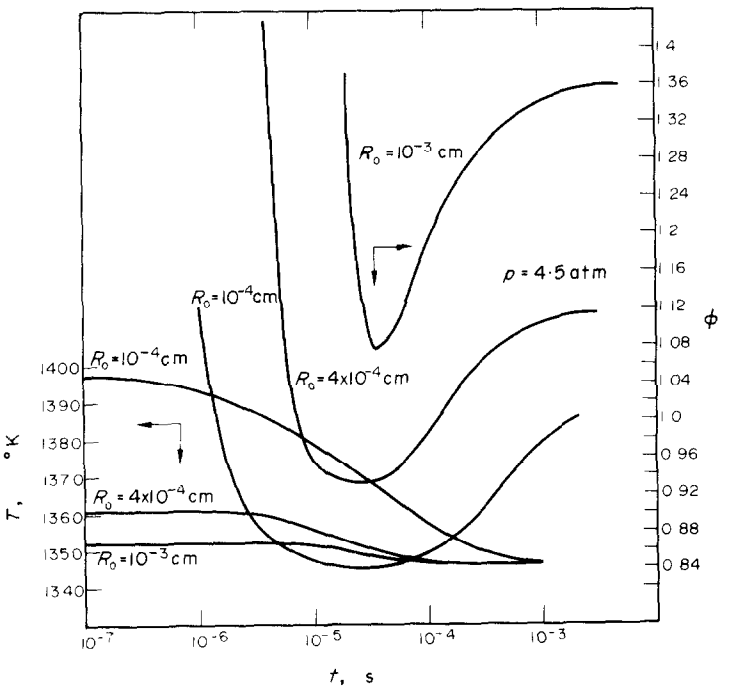


FIG. 12. $\phi$, $T$ vs $t$ for $p = 4{\cdot}5$ atm, $R_0 = 10^{-4}, 4 \times 10^{-4}, 10^{-3}$ cm.

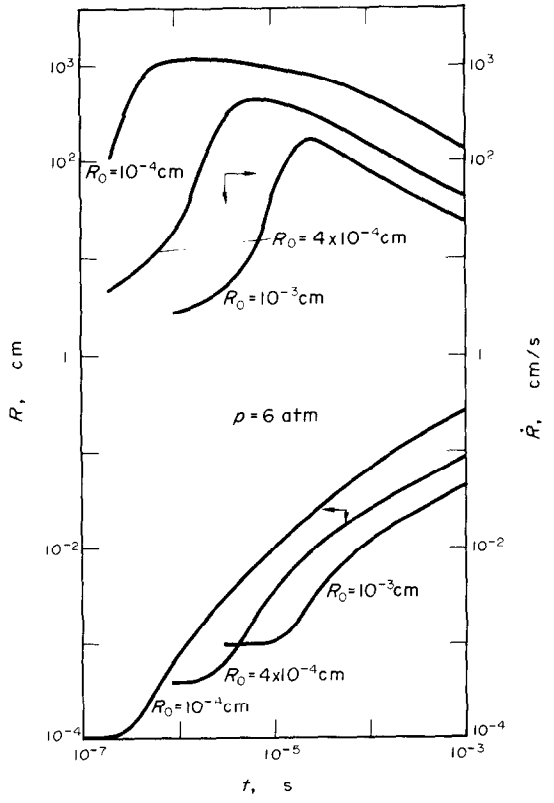


FIG. 13. $R$, $\dot{R}$ vs $t$ for $p = 6$ atm, $R_0 = 10^{-4}, 4 \times 10^{-4}, 10^{-3}$ cm.

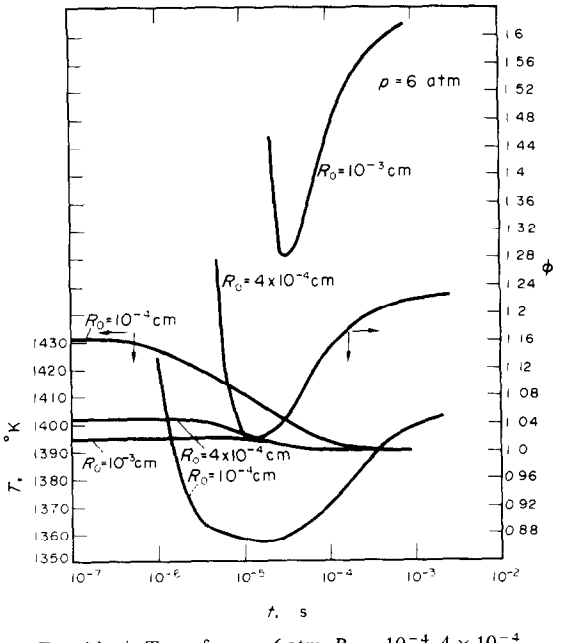


FIG. 14. $\phi$, $T$ vs $t$ for $p = 6$ atm, $R_0 = 10^{-4}, 4 \times 10^{-4}, 10^{-3}$ cm.

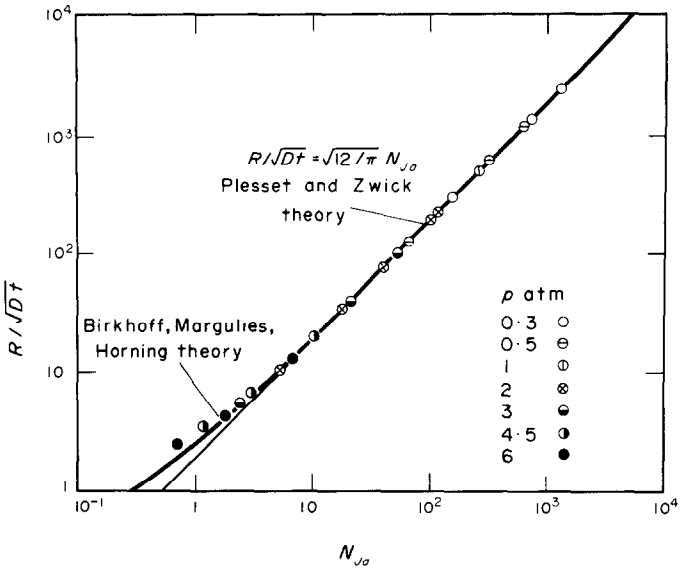


FIG. 15. Comparison of results obtained with HY-BUBBLE in the asymptotic region and analytical asymptotic solutions.

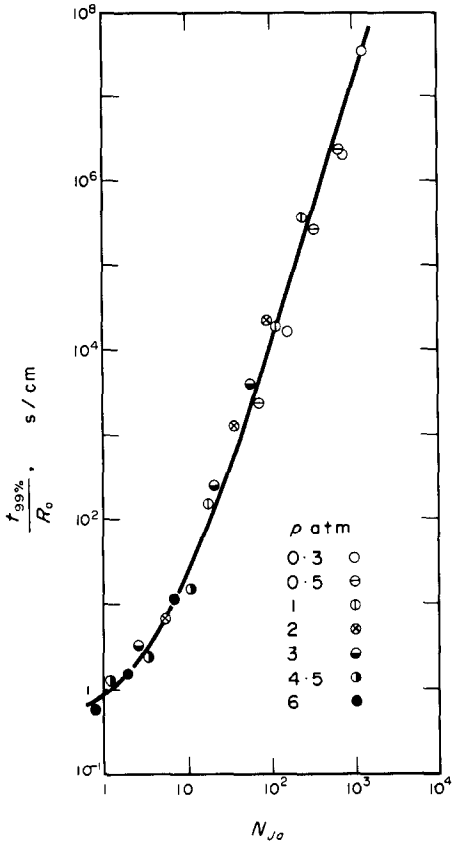


FIG. 16. $t_{99\%}/R_0$ vs $N_{Ja}$.

Figure 16 shows the ratio of $t_{99\%}$ (time required to reach $\phi = 0{\cdot}99$, that is a bubble radius differing less than 1 per cent from the asymptotic Plesset–Zwick solution) to the initial bubble radius $R_0$ vs the Jakob number. The points are correlated rather well by a single line. For high Jakob numbers this ratio increases exponentially with $N_{Ja}$. This means that for sodium with high degrees of superheating the asymptotic solution has no practical importance, because it becomes valid only for unrealistically big bubbles.

Table 1 shows in schematic form the main results of the present calculations.

## 6. COMPARISON WITH THE DATA OF OTHER AUTHORS

Figure 17 shows the experimental data of Cole and Shulman with the highest degree of superheat [20]. The Plesset–Zwick asymptotic solution predicts bubble radii which are much too large. The present analysis agrees better with experiment, however the analysis still overpredicts the size of the bubble. One obvious reason for this discrepancy is the fact that we assume in the calculation a constant value of $T_0$ equal to the wall temperature $T_w$. In reality the bubble originates at the wall, but, as soon as it expands, it comes in contact with liquid layers at lower temperatures. The liquid temperature approaches the saturation temperature away from the wall and a better approximation of the experiment might be to assume $T_0 = \frac{1}{2}(T_w + T_s)$. Figure 17 shows that, indeed, in this case the agreement

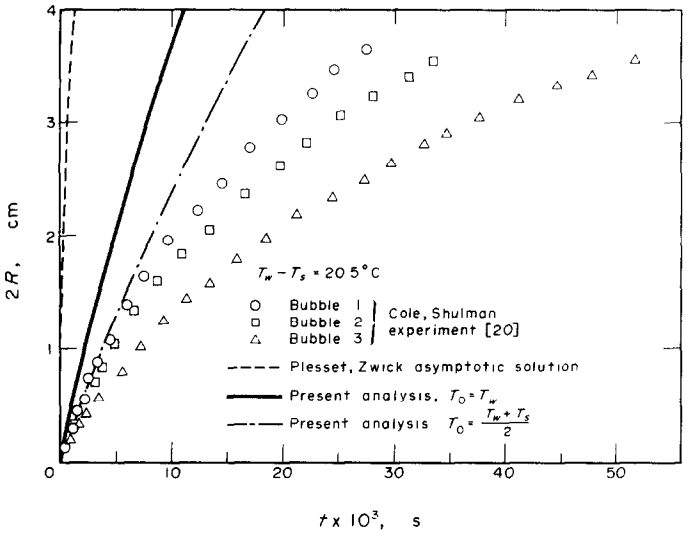


FIG. 17. Comparison of present analysis and Cole–Shulman's experiments.

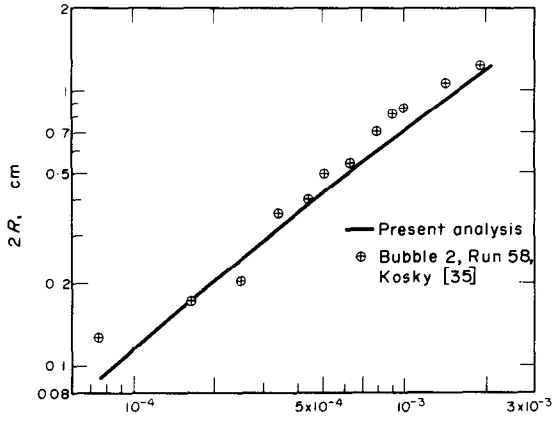


FIG. 18. Comparison of present analysis and Kosky's experiments.

between experiment and calculation is better. However for bubble diameters greater than 1 cm the bubbles are still smaller than the predicted values. This is probably due to their coming into contact with liquid at temperatures even lower than $\frac{1}{2}(T_w + T_s)$.

Figure 18 shows the experimental data obtained by Kosky with water [35] in the case of the bubble with the highest superheat (36°C). The data agree well with our analysis. This is of course also the case for the other experiments of Kosky at lower superheats. This good agreement is probably due to the fact that the bubbles are not very big and the assumption of constant temperature of the undisturbed surrounding liquid is good. Furthermore, care was taken during this experiment to have water particularly pure and deprived of dissolved gases. As shown in Fig. 19 the data of Hooper and Abdelmessih for large superheats

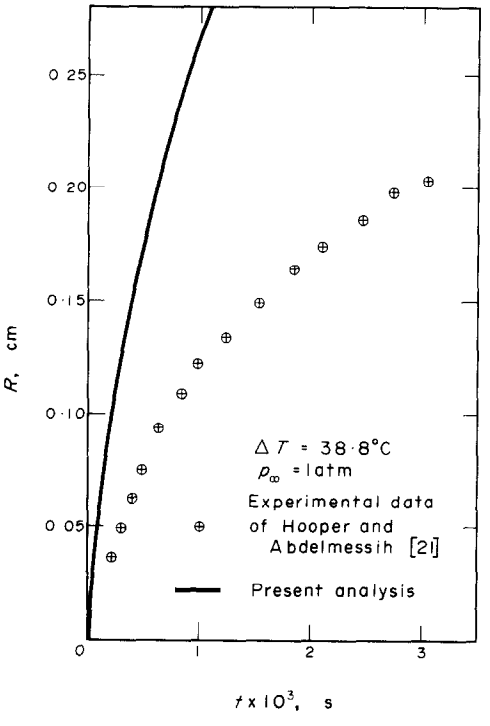


FIG. 19. Comparison of present analysis and Hooper–Abdelmessih's experiments.

[21] do not agree well with our analysis. This could be given by gas dissolved in the water or could be due to nonequilibrium effects which we will discuss below.

In 1969, when part of the present work had been already performed, Fauske, Theofanous, Biasi and Isbin [36] published the results of calculations similar to those of the present work. The main difference from

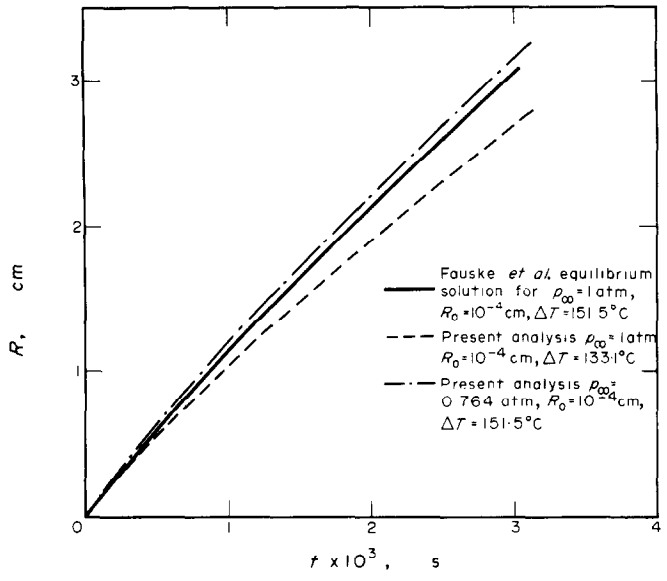


FIG. 20. Comparison of present with Fauske *et al.* analysis.

the present work is that they did not solve the energy equation in the liquid as we did, but they simply assumed a quadratic distribution of temperature in the liquid surrounding the bubble. Figure 20 shows the calculation performed by Fauske *et al.* for $p_\infty = 1$ atm, $R_0 = 10^{-4}$ and $\Delta T = T_0 - T_s = 151{\cdot}5°C$. Due probably to slightly different assumed sodium properties we obtain, for the same $p_\infty$ and $R_0$, $T_0 - T_s = 133{\cdot}1°C$ and therefore bubbles about 13 per cent smaller. The results of Fauske *et al.* however, compare well with ours for $R_0 = 10^{-4}$ and $T_0 - T_s = 151{\cdot}5°C$, for which we have to assume $p_\infty = 0{\cdot}764$ atm.

Fauske *et al.* consider also a coefficient $c$ which takes into account the nonequilibrium effects at the vapor–liquid boundary surface (for equilibrium conditions $c = \infty$). The data of Hooper and Abdelmessih can be matched by their analytical data at least up to $t = 10^{-3}$ s by assuming $c = 10^{-2}$. As we have shown, however, the experimental data of Cole and Shulman and those of Kosky agree well with our analytical equilibrium solution.

*Acknowledgements*—The authors wish to thank Dr J. Merkwitz who suggested the transformation given by equation (30) and Mr M. Küchle for the calculation of the energy release of the radiation particles in sodium. They also acknowledge the help of Dr C. Savatteri who made some of the calculations with HY-BUBBLE.

## REFERENCES

1. D. V. Bugg, The bubble chamber, *Progr. Nucl. Phys.* **7**, 2–52 (1958).
2. F. Seitz, On the theory of the bubble chamber, *Physics Fluids* **1**, 2–13 (1958).
3. J. A. Ghormley, Nucleation of bubbles in superheated aqueous solutions by fast particles, *J. Nucl. Energy* **6**, 300–302 (1958).
4. A. Norman and P. Spiegler, Radiation nucleation of bubbles in water, *Nucl. Sci. Engng* **16**, 213–217 (1963).
5. M. S. Plesset and S. A. Zwick, A nonsteady heat diffusion problem with spherical symmetry, *J. Appl. Phys.* **23**, 95–98 (1952).
6. M. S. Plesset and S. A. Zwick, The growth of vapor bubbles in superheated liquids, *J. Appl. Phys.* **25**, 493–500 (1954).
7. H. K. Foster and N. Zuber, Growth of a vapor bubble in a superheated liquid, *J. Appl. Phys.* **25**, 474 (1954).
8. S. A. Zwick and M. S. Plesset, On the dynamics of small vapor bubbles in liquids, *J. Math. Phys.* **33**, 308–330 (1955).
9. G. Birkhoff, R. S. Margulies and W. A. Horning, Spherical bubble growth, *Physics Fluids* **1**, 201–204 (1958).
10. L. E. Scriven, On the dynamics of phase growth, *Chem. Engng Sci.* **10**(1/2), 1 (1959).
11. S. G. Bankoff, Bubble dynamics in boiling, in *Conf. on Boiling and Two Phase Flow for Heat Transfer Engineers*, Berkeley, Gmelin-AED-Conf. 124–15 (1965).
12. P. Dergarabedian, The rate of growth of vapor bubbles in superheated water, *J. Appl. Mech.* **75**, 537–545 (1953).
13. H. W. Hoffmann and A. I. Krakoviak, Convective boiling with liquid potassium, in *Proc. 1964 Heat Transfer and Fluid Mechanics Institute*. Stanford University Press, Stanford, Calif. (1964).
14. J. A. Edwards and H. W. Hoffmann, Superheat with boiling alkali metals, in *Proc. Fourth High-temperature Liquid-Metal Heat Transfer Technology Conf.*, Argonne National Laboratory (1965).
15. K. H. Spiller, G. Grass and D. Perschke, Überhitzung und Einzelblasenejektion bei der Verdampfung von stagnierenden Flüssigmetallen, *Atomkernenergie* **12**, 111–114 (1967).
16. M. Dalle Donne and S. Dorner, Karlsruhe internal report (1967).

17. W. Peppler, Karlsruhe internal report (1967).
18. E. G. Schlechtendahl, Die Ejektion von Natrium aus Reaktorkühlkanälen, *Nukleonik* **10**, 270–274 (1967).
19. A. M. Judd, Boiling and condensation of sodium in relation to fast reactor safety, in *Proc. International Conf. on Safety of Fast Reactors*, Aix-en-Provence (1967).
20. R. Cole and H. Shulman, Bubble Growth rates at high Jakob numbers, *Int. J. Heat Mass Transfer* **9**, 1377–1390 (1966).
21. F. C. Hooper and A. H. Abdelmessih, The flashing of liquids at higher superheats, in *Proc. Third International Heat Transfer Conf. ASME–AIChE*, Chicago (August 1966).
22. M. Dalle Donne, A new and simple method of estimating the liquid superheat due to surface conditions in nucleate boiling and its application to sodium, *Nukleonik* **8**, 133–137 (1966) and KFK 425.
23. E. L. Dunning, The thermodynamic and transport properties of sodium and sodium vapor, ANL-6246 (1960).
24. Lord Rayleigh, *The Theory of Sound*, 2nd edn. Dover, New York (1945).
25. R. D. Birkhoff, *Handb. Physik* **34**, 99 (1958).
26. W. Whaling, *Handb. Physik* **34**, 209 (1958).
27. Segre and Wiegand, *Phys. Rev.* **70**, 808 (1964).
28. K. T. Claxton, The influence of radiation on the inception of boiling in liquid sodium, in *Proc. International Conf. on Safety of Fast Reactors*, Aix-en-Provence (1967).
29. S. Goldstein (ed.), *Modern Developments in Fluid Dynamics*, Vol. 1. Clarendon Press, Oxford (1952).
30. Lord Rayleigh, On the pressure developed in a liquid during the collapse of a spherical cavity, *Phil. Mag.* **34**, 94–98 (1917).
31. I. Babuska, M. Prager and E. Vitasek, *Numerical Processes in Differential Equations*, Chapter 6.1. SNTL, Prague (1966).
32. R. Varga, *Matrix Iterative Analysis*, Chapter 6.4. Prentice Hall, Englewood Cliffs, N.J. (1965).
33. W. L. Wilkinson, Error analysis of direct methods of matrix inversion, *J. Assoc. Comput. Mach.* **8**, 281–330 (1961).
34. E. G. Schlechtendahl, Sieden des Kühlmittels in natriumgekühlten schnellen Reaktoren, KFK 1020 (1969).
35. P. G. Kosky, Bubble growth measurements in uniformly superheated liquids, *Chem. Engng Sci.* **23**, 695–706 (1968).
36. H. Fauske, T. Theofanous, L. Biasi and H. S. Isbin, A theoretical study on bubble growth in constant and time dependent-pressure fields, *Chem. Engng Sci.* **24**(3), 885 (1969).
37. M. Sittig, *Sodium, Its Manufacture, Properties and Uses*. Reinhold, New York (1956).
38. *VDI-Wärmeatlas*, Db3, Berlin (1953).
39. N. B. Vargaftik and A. A. Tarzimanov, *Teploenergetika* **8**(6), 5–8 (1961).
40. M. P. Voukalovitch, *Thermodynamic Properties of Water and Steam*. VEB, Berlin (1958).
41. M. P. Voukalovitch *et al.*, *Teploenergetika* **8**(12) (1962).
42. *VDI-Wärmeatlas*, Db2, Berlin (1953).
43. *Handbook of Chemistry and Physics*, p. 2239, 44th edn. The Chemical Rubber Publishing Co., Cleveland, Oh. (1962–1963).
44. H. Vesper, Näherungsgleichungen für die Zustandsgrößen des Wassers und des Dampfes an der Grenzkurven zur Verwendung in elektronischen Rechenmaschinen, Brennst.-Wärme-Kraft **15**, 20–23 (1963).
45. H. G. Franze, Internal Kernforschungszentrum Report.

## APPENDIX 1
### *Physical Properties*

A.1. *Sodium*

The assumed properties for sodium were the following:

$$k[\text{cal/cm s °K}] = 0{\cdot}2482 - 1{\cdot}16\times10^{-4}T\ [23] \tag{49}$$

$$\rho[\text{g/cm}^3] = 1{\cdot}0086 - 2{\cdot}134\times10^{-4}T - 1{\cdot}75\times10^{-8}T^2\ [23] \tag{50}$$

$$c[\text{cal/g °K}] = 0{\cdot}38966 - 1{\cdot}9917\times10^{-4}T + 1{\cdot}105\times10^{-7}T^2\ [37] \tag{51}$$

$$D[\text{cm}^2/\text{s}] = \frac{k}{\rho c_p} \tag{52}$$

$$\sigma[\text{dyn/cm}] = 229{\cdot}3 - 0{\cdot}1T\ [23] \tag{53}$$

$$\mu[\text{g/cm s}] = 10^{-3\ 09127+(382/T+40)}\ [37] \tag{54}$$

$$p_v[\text{dyn/cm}^2] = \frac{10^{6{\cdot}354-(5567/T)}}{9{\cdot}8692\times10^{-7}\sqrt{T}}\ [23] \tag{55}$$

$$\frac{L\rho_v}{k}[\text{s °K/cm}^2] = A' + B'T \tag{56}$$

with

$$A' = 309{\cdot}7198 - 1653{\cdot}496\times10^{-6}T^2 + 2149{\cdot}768\times10^{-9}T^3 - 810{\cdot}084\times10^{-12}T^4$$

$$B' = -1{\cdot}157965 + 3306{\cdot}992\times10^{-6}T - 3224{\cdot}652\times10^{-9}T^2 + 1080{\cdot}112\times10^{-12}T^3$$

$$\frac{1}{3k}\frac{\partial(L\rho_v)}{\partial T}[\text{s/cm}^2] = B = \frac{7{\cdot}19547\times10^{-3} - 1{\cdot}6288\times10^{-5}T + 9{\cdot}2759\times10^{-9}T^2}{0{\cdot}2482 - 1{\cdot}16\times10^{-4}T} \tag{57}$$

$$\frac{2\sigma}{3Jk}[\text{s °K/cm}] = A'' + B''T$$

with

$$A'' = 0{\cdot}1232\times10^{-4}, \qquad B'' = 0{\cdot}30933\times10^{-8} \tag{58}$$

$$\frac{1}{3Jk}\frac{\partial\sigma}{\partial T}[\text{s/cm}] = C = \frac{A''}{k} = \frac{-0{\cdot}7963\times10^{-9}}{0{\cdot}2482 - 1{\cdot}16\times10^{-4}T}. \tag{59}$$

Equations (56), (57) and (58) have been obtained by fitting polynomial expressions to the tabulated values of $L$, $\rho_v$, $k$ and $\sigma$ from [23], the error being less than 1·5 per cent in the pertinent temperature range of 1000°K $\leqslant T \leqslant$ 1600°K.

A.2. *Water*

The assumed properties for water were the following:

$$k[\text{cal/cm s °K}] = 2{\cdot}778\times10^{-3}\{0{\cdot}4775 - 8{\cdot}33\times10^{-6}(T-273)^2 + 0{\cdot}191\times10^{-2}.(T-273) + 4\times10^{-5}p_\infty[\text{kg/cm}^2]\} \text{ for } T \leqslant 373\text{°K} \tag{60}$$

$$k[\text{cal/cm s °K}] = 2{\cdot}778\times10^{-3}\{0{\cdot}5125 - 4{\cdot}53\times10^{-6}(T-273)^2 + 0{\cdot}1187\times10^{-2}.(T^{-273}) + 7\times10^{-5}p_\infty[\text{kg/cm}^2]\} \text{ for } T > 373\text{°K}\ [38, 39]$$

$$\rho[\text{g/cm}^3] = \{3{\cdot}086 - 0{\cdot}889017(101-T)^{0{\cdot}147166} - 0{\cdot}39(111{\cdot}9-T)^{-1{\cdot}6}\times(p_\infty[\text{kg/cm}^2] - 225{\cdot}5)\}^{-1}\ [40] \tag{61}$$

Table 1

| $p_\infty$ (atm) | $R_0$ (cm) | $T_s$ (°K) | $T_0 - T_s$ (°K) | $\frac{R}{\sqrt{(Dt)}}$ for $t \to \infty$ | $N_{Ja}$ | $t_{99\%}$ (s) | $\frac{t_{99\%}}{R_0}$ (s/cm) |
|---|---|---|---|---|---|---|---|
| 0·3 | $2·5 \times 10^{-5}$ | 1036·9 | 382·9 | 2500 | 1293 | 834 | $3·34 \times 10^{7}$ |
| | $10^{-4}$ | | 218·7 | 1302 | 681 | 215 | $2·15 \times 10^{6}$ |
| | $10^{-3}$ | | 53·6 | 307 | 157 | 16 | $1·6 \times 10^{4}$ |
| 0·5 | $2·5 \times 10^{-5}$ | 1083·6 | 340·1 | 1274 | 650 | 56 | $2·24 \times 10^{6}$ |
| | $10^{-4}$ | | 181·6 | 635 | 325 | 26·2 | $2·62 \times 10^{5}$ |
| | $10^{-3}$ | | 37·7 | 124 | 63·7 | 2·28 | $2·28 \times 10^{3}$ |
| 1 | $2·5 \times 10^{-5}$ | 1154·6 | 278·9 | 509 | 261 | 8·7 | $3·48 \times 10^{5}$ |
| | $10^{-4}$ | | 133·1 | 226 | 116 | 1·9 | $1·9 \times 10^{4}$ |
| | $10^{-3}$ | | 22·1 | 36·2 | 18·2 | 0·14 | $1·4 \times 10^{2}$ |
| 2 | $2·5 \times 10^{-5}$ | 1235·2 | 216·0 | 200 | 102 | 0·52 | $2·08 \times 10^{4}$ |
| | $10^{-4}$ | | 90·1 | 78·3 | 39·9 | 0·119 | $1·19 \times 10^{3}$ |
| | $10^{-3}$ | | 12·4 | 11·0 | 5·28 | $6·2 \times 10^{-3}$ | 6·2 |
| 3 | $2·5 \times 10^{-5}$ | 1288·1 | 179·9 | 114 | 58·2 | $9·14 \times 10^{-2}$ | $3·66 \times 10^{3}$ |
| | $10^{-4}$ | | 69.0 | 41·4 | 20·9 | $2·4 \times 10^{-2}$ | $2·4 \times 10^{2}$ |
| | $10^{-3}$ | | 8·71 | 5·75 | 2·54 | $3 \times 10^{-3}$ | 3 |
| 4·5 | $10^{-4}$ | 1345·9 | 51·4 | 20·9 | 10·7 | $1·44 \times 10^{-3}$ | 14·4 |
| | $4 \times 10^{-4}$ | | 14·7 | 6·52 | 2·99 | $9·2 \times 10^{-4}$ | 2·3 |
| | $10^{-3}$ | | 6·06 | 3·24 | 1·22 | $1·13 \times 10^{-3}$ | 1·13 |
| 6 | $10^{-4}$ | 1390·2 | 41·0 | 13·5 | 6·60 | $1·06 \times 10^{-3}$ | 10·6 |
| | $4 \times 10^{-4}$ | | 11·4 | 4·29 | 1·79 | $6 \times 10^{-4}$ | 1·5 |
| | $10^{-3}$ | | 4·66 | 2·28 | 0·72 | $6·4 \times 10^{-4}$ | 0·64 |

$$c[\text{cal/gr °K}] = 1·005 - 4·47 \times 10^{-4}(T-273) + 3·92 \times 10^{-6}(T-273)^2 \text{ [41, 42]} \quad (62)$$

$$D[\text{cm}^2/\text{s}] = \frac{k}{\rho c} \quad (63)$$

$$\sigma[\text{dyn/cm}] = 76 - 0·171(T-273) \text{ [43]} \quad (64)$$

$$\frac{\mu}{\rho}[\text{cm}^2/\text{s}] = 10^{-2}\left(0·03 + \frac{30}{T-273} - \frac{250}{(T-273)^2}\right) \text{[40, 42]} \quad (65)$$

$$p_v[\text{dyn/cm}^2] = 9·806 \times 10^5 \, e^{\sum_{n=0}^{9} a_n \left(\frac{T-273}{100}\right)^n} \text{ [44]} \quad (66)$$

with

$a_0 = -5·078709984$ $\quad a_5 = +2·477563380 \times 10^{-1}$
$a_1 = +7·270489907$ $\quad a_6 = -8·659024966 \times 10^{-2}$
$a_2 = -3·033726807$ $\quad a_7 = +2·015339284 \times 10^{-2}$
$a_3 = +1·256759065$ $\quad a_8 = -2·693452728 \times 10^{-3}$
$a_4 = -5·608659370 \times 10^{-1}$ $\quad a_9 = +1·553179872 \times 10^{-4}$

$$\frac{L\rho_v}{k}[\text{s °K/cm}^2] = A' + B'(T-273) \text{ [38–40]}$$

with

$$A' = -58·66 + 549·01 \times 10^{-4}(T-273)^2 - 926·58 \times 10^{-6}(T-273)^3 \quad (67)$$

$$B' = 3·411 - 1098·2 \times 10^{-4}(T-273) + 1389·87 \times 10^{-6}(T-273)^3$$

$$\frac{1}{3k}\frac{\partial(L\rho_v)}{\partial T}[\text{s/cm}^2] = B = \frac{0·1628 \times 10^{-3} - 0·544 \times 10^{-4}(T-273) + 0·73067 \times 10^{-6}(T-273)}{k} \text{ [38–40]} \quad (68)$$

$$\frac{2\sigma}{3Jk}[\text{s °K/cm}] = A'' + B''(T-273) \text{ [38–40]}$$

with

$$A'' = 2·439 \times 10^{-2}$$
$$B'' = -0·6990 \times 10^{-4}(T-273) \quad (69)$$

$$\frac{1}{3Jk}\frac{\partial\sigma}{\partial T}[\text{s/cm}] = C = \frac{A'''}{k} = \frac{-0·13617 \times 10^{-8}}{k}. \quad (70)$$

Equations (60), (62), (65) have been obtained in [45] by fitting polynomial expressions to the numerical data presented in table form in the references given for each equation. Equations (67), (68) and (69) have been obtained by fitting polynomial expressions to the numerical values of $L\rho_v/k$, $L\rho_v$ and $\sigma/k$ from the references given for each equation, the error being less than 1·5 per cent in the range 40–140°C.